STRUCTURAL INSIGHT INTO PROTEIN KINASE D SMALL MOLECULE INHIBITION

by

Evan J. Carder

Bachelor of Science, University of Pittsburgh, 2011

Submitted to the Graduate Faculty of

The University of Pittsburgh School of Medicine

in partial fulfillment of the requirements for the degree of

Master of Science

University of Pittsburgh

2014

UNIVERSITY OF PITTSBURGH

SCHOOL OF MEDICINE

This thesis was presented

by

Evan J. Carder

It was defended on

August 15, 2014

and approved by

Committee Chair: Guillermo Romero, Ph.D
Associate Professor, Associate Director of Molecular Pharmacology Program
Department of Pharmacology and Chemical Biology

Yu Jiang, Ph.D
Associate Professor
Department of Pharmacology and Chemical Biology

Jing Hu, Ph.D
Assistant Professor
Department of Pharmacology and Chemical Biology

Thesis Advisor: Qiming Jane Wang, Ph.D
Associate Professor, Vice Chair of Regulatory Affairs
Department of Pharmacology and Chemical Biology

STRUCTURAL INSIGHT INTO PROTEIN KINASE D SMALL MOLECULE INHIBITION

Evan J. Carder, M.S.

University of Pittsburgh, 2014

Protein kinase D (PKD) is a family of serine/threonine kinases that has emerged as a novel therapeutic target in multiple diseases; therefore, the development of small molecule inhibitors that abrogate PKD's function has been an area of intense investigation. However, these efforts have not yet resulted in a PKD therapeutic that is available for clinical applications. Access to structural information can greatly accelerate this drug discovery process and allow future initiatives to benefit from structure-based drug design. Therefore, we employed both computational and experimental methods to investigate the important characteristics of PKD small molecule inhibitors that allow for excellent potency and selectivity. We found that type I ATP-competitive PKD inhibitors bind to the hinge region and position a hydrogen bond acceptor near the charged side chain of Lys612. An additional moiety (typically a basic amino group) capable of developing a critical salt bridge with Glu710 was shown to be important for improved affinity. Further analysis from inhibitor selectivity profiles suggested strategic functionalization in pocket II could potentially reduce kinase off-target effects. From our experimental investigation of CRT0066101 inhibition, we developed a chemical genetic tool kit for evaluating PKD function. Mutating the gatekeeper residue, Met659, to phenylalanine or tyrosine dramatically sensitized PKD to CRT0066101 inhibition. Conversely, mutating hinge residue, G664, to valine or isoleucine conferred resistance. Taken together, our study provides key insights into the chemical features associated with PKD inhibition, which will aid in the future development of a novel PKD therapeutic.

TABLE OF CONTENTS

LIST OF TABLES

LIST OF FIGURES

AWKNOWLEDGEMENTS

I would like to thank Dr. Qiming Jane Wang for providing me the opportunity to work in her laboratory. I am very grateful for the training I received during my time in her group. Additionally, I would like to express my appreciation to Dr. Wang lab members for their scientific support and friendship.

I would also like to sincerely thank Dr. Guillermo Romero for his mentorship and scientific support. I thank Dr. Yu Jiang and Dr. Jing Hu for serving on my committee. Additionally, I want to thank the Molecular Pharmacology program and the Department of Pharmacology and Chemical Biology for financial support and providing me with an opportunity to establish a strong foundation in drug discovery.

Most of all, I express my deepest gratitude to my friends and family for their unconditional love and support during my graduate studies.

1.0 INTRODUCTION

1.1 PROTEIN KINASE D

1.1.1 Protein Structure and Regulation

Protein kinase D (PKD) is a family of serine/threonine kinases that were discovered during an exciting era when novel kinases were being explored and implicated in a diverse array of important signaling events[1, 2]. Since its discovery, the investigation into PKD's regulation and function has led to a rich source of insight into a broad range of biological processes. The three isoforms of PKD identified, PKD1/PKCμ[1, 3], PKD2[4], and PKD3/PKCν[5], were initially classified as atypical protein kinase Cs (aPKCs); however, they were later grouped into a subfamily of the calcium/calmodulin-dependent protein kinase (CAMK) superfamily due to greater sequence homology in their catalytic domain. PKD's general structure consists of three central domains bifurcated into the regulatory region and catalytic region (Figure 1). Located near the N-terminus, PKD's regulatory region plays a critical role in cellular localization, protein-protein interaction, and autoinhibition. Specifically, the tandem cysteine-rich domains (CRD) named C1a and C1b bind to second messenger diacyl glycerol (DAG) or DAG analogs phorbol esters and facilitate PKD localization at the plasma membrane, mitochondria, and Golgi[6-9]. The pleckstrin homology (PH) domain, which is absent in PKC family members, is commonly

associated with inter- and intramolecular interactions and protein localization[10]. In the context of PKD regulation, the CRD and PH domain are responsible for autoinhibition. Mutations at select residues or deletion of either the CRD or PH domain leads to an active protein[11,12]. Positioned near the C-terminus, the catalytic region contains the kinase domain, which is responsible for PKD's enzymatic function. Activation of PKD's kinase domain is due to PKC-mediated transphosphorylation of serine residues found within PKD's activation loop[13]. Subsequent autophosphorylation at the C-terminus results in prolonged enzymatic activity[14-17].

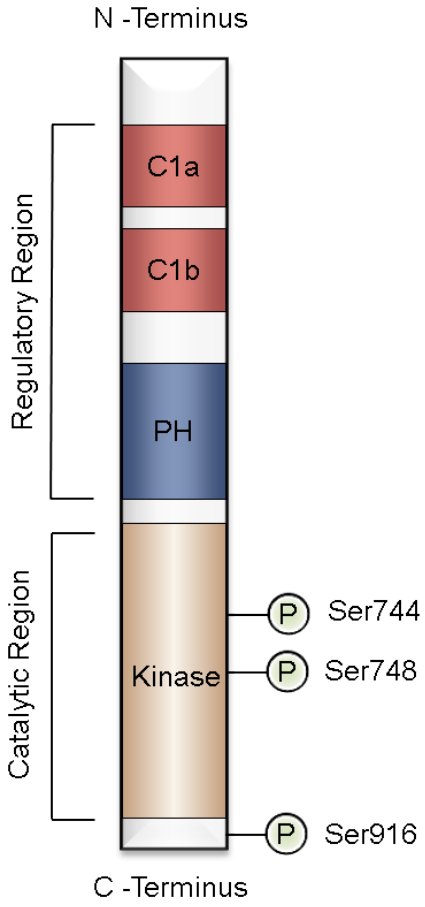

Figure 1. Linear representation of Protein Kinase D

1.1.2 Signaling in Disease Phenotypes

PKD is integrated in multiple signaling pathways (Figure 2). Acting downstream of G-protein coupled receptors (GPCR) as well as receptor and non-receptor tyrosine kinases, PKD response is associated with a number of different stimuli - GPCR agonists, growth factors, oxidative stress, and UV-B radiation[18-23]. Activation of phospholipase C (PLC) and subsequent hydrolysis of phosphatidylinositol 4,5-biphosphate generates second messengers Ins $(1,4,5)P_3$ and DAG. In turn, DAG binds to PKD's cysteine-rich domain and induces PKD translocation from the cytosol to the cell membrane[7, 24, 25]. Following PKC-mediated transphosphorylation of PKD's activation loop at Ser744/Ser748, PKD autoinhibition is relieved, thereby, yielding an active kinase[13, 15, 26]. Consequently, PKD rapidly translocates back to the cytosol where it can reach various subcellular compartments to propagate key signaling events from the cell surface[24].

PKD regulates many important signaling pathways that are essential in DNA synthesis and cell proliferation. It has been shown that PKD modulates the mitogen-activated protein kinase (MAPK) signaling pathway. Aberrant MAPK signaling is associated in the development of multiple types of cancer, making it a valid target for anticancer therapeutics[27]. The Ras and Rab interactor 1 (RIN1) protein, in its unphosphorylated form, competes with Raf to inhibit the Ras/Raf interaction, thereby reducing downstream MEK/ERK signaling. PKD1 can phosphorylate RIN1 at Ser351, resulting in its binding to 14-3-3 proteins and subsequent sequestration to the cytosol, thereby, impeding its ability to negatively regulate Ras/Raf[28]. Thus, PKD facilitates sustained stimulation of ERK and consequently c-Fos activity, which can lead to increased DNA synthesis and cell proliferation[29, 30]. Overexpression of PKD resulted in prolonged ERK activation in various cancer cells[31], providing a potential mechanism through which PKD contributes to tumor growth.

PKD affects gene expression by acting on class IIa histone deacetylases (HDAC4, 5, 7, and 9). HDACs are important epigenetic regulators that control chromatin structure. Deacetylation of histones results in enhanced transcriptional repression and reduced gene expression. Aberrant class IIa HDACs have been associated in the deregulation of multiple signaling events and implicated in adverse phenotypes[32]. Investigations into cardiovascular disease found HDAC5 and HDAC9 negatively regulate cardiac hypertrophy by repressing the transcription factor myocyte enhancer factor 2 (MEF2). PKD directly phosphorylates class IIa HDACs and facilitates their complex formation with 14-3-3 proteins, leading to HDAC nuclear exclusion and sequestration in the cytoplasm, thereby de-repressing MEF2 activity and resulting in the expression of target genes[33]. In neonatal rat ventricular myocytes, PKD-induced phosphorylation of HDAC5 led to MEF2-mediated transcription of genes implicated in cardiac hypertrophy and heart failure. Additionally, transgenic mice with PKD1-defecient cardiomyocytes were resistant to cellular hypertrophy following stimulation by angiotensin II, isoprotenerol, or pressure-induced overload.

NF-κB is a key transcription factor associated in the expression of multiple genes that regulate cell surivival and immune response. In the presence of oxidative stress, PKD is recruited to the mitochondria and activated through phosphorylation of its PH domain and activation loop by Src-Abl tyrosine kinase and PKCδ, respectively[34-36]. This leads to PKD-mediated phosphorylation of inhibitory κ kinase (IKK) and the concomitant degradation of IκB. NF-κB released from the inhibitory complex subsequently accumulates in the nucleus and induces gene expression. As a result, the generation of manganese-dependent superoxide dismutase (MnSOD) aids in cellular detoxification and reduces the risk of cell death. In addition, PKD was also shown to support cell survival by influencing the c-Jun N-terminal kinase (JNK)

pathway[37]. Like NF-κB, c-Jun is a transcription factor associated in stress response. PKD is able to phosphorylate c-Jun at its N-terminus and suppress JNK-mediated c-Jun activation, which inhibits apoptosis[38, 39].

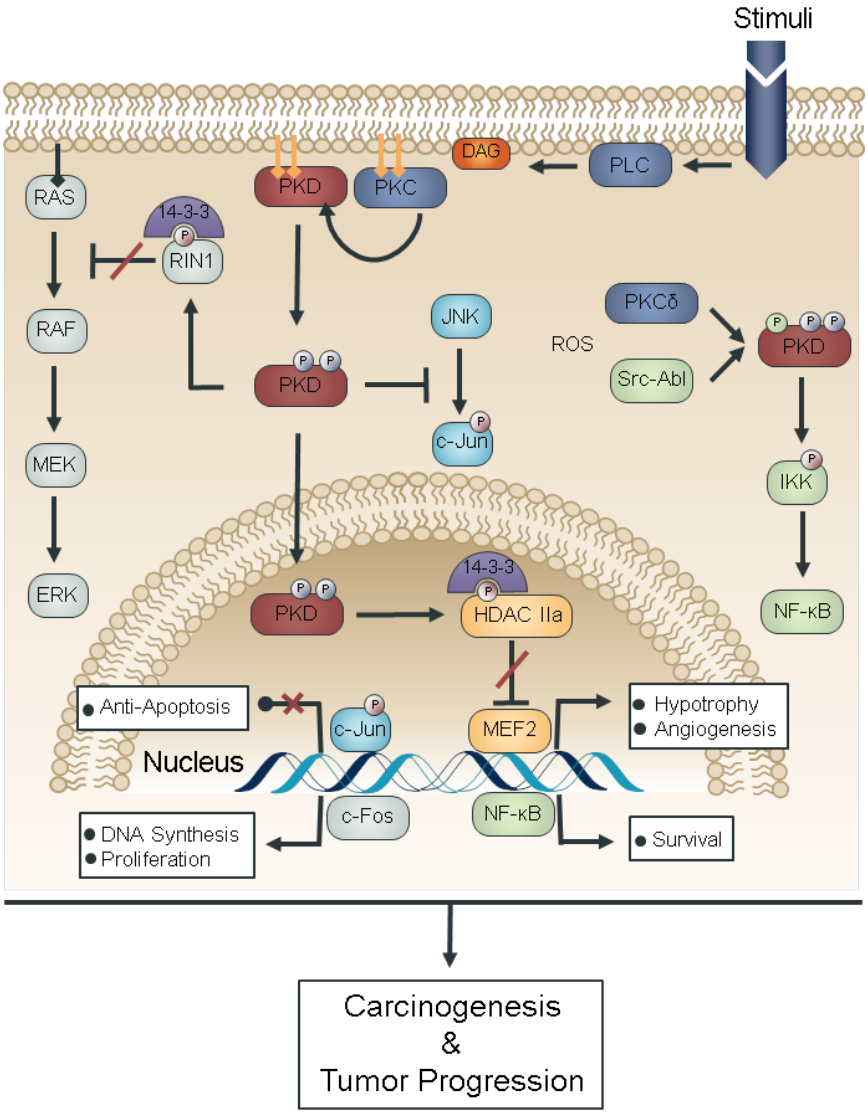

Figure 2. PKD signaling in disease phenotypes

1.1.3 Targeted Pharmacological Agents

Given its role in integrating upstream signaling pathways, PKD is associated in a multitude of biological processes. Deregulation of PKD can lead to abnormal activity of multiple cellular events, resulting in a broad array of disease phenotypes such as increased DNA synthesis, cell proliferation, angiogenesis, hypertrophy, and promote anti-apoptotic and survival mechanisms (Figure 2). Therefore, PKD may be a promising therapeutic target. Thus, in an effort to further investigate PKD, drug discovery programs has provided a number of PKD pharmacological agents.

Early investigations into PKD inhibition explored various pan-kinase inhibitors. Among those reported, indolocarbazole natural products like staurosporine and its anologs were shown to target PKD with low nanomolar concentrations; however, these compounds were also recognized as potent PKC inhibitors[40]. Further studies revealed resveratrol, a stilbenoid natural product known for its antioxidant and chemopreventive properties, inhibited PKD as well as other protein kinases at micromolar concentrations[41]. Both classes of inhibitors were highly investigated and showed antitumor activity in animal models; although, their poor selectivity limited their ability to evaluate PKD in a cellular context. This considerable challenge led to the pursuit of PKD-targeted agents (Table 1).

Table 1. Targeted protein kinase D inhibitors

Name	Mechanism	Disease Model	Enzyme IC_{50} (nM)	Cellular EC_{50} (uM)	F (%)
CID755673	Non-ATP Competitive	Prostate Cancer	182	11.8	-
KB-Nb142-70	Non-ATP Competitive	Prostate Cancer	28	2.2	-
KMG-Nb4-23	Non-ATP Competitive	Prostate Cancer	120	6.8	-
NPKDi	ATP-Competitive	Cardiac Hypotrophy	0.6	0.032	4
BPKDi	ATP-Competitive	Cardiac Hypotrophy	1	0.077	-
CRT0066101	ATP-Competitive	Pancreatic Cancer	0.7	0.5	100
CRT0066051	ATP Competitive	Angiogenesis	0.4	0.2	-
Roche 139	ATP Competitive	Prostate Cancer	16.8	1.5	-
SD208	ATP Competitive	Prostate Cancer	106	17	-

CID755673 was the first PKD-specific inhibitor to be reported (Figure 3). Possessing a structurally novel benzoxoloazepinolone scaffold, CID755673 inhibited PKD1 at approximately 182 nM[42]. Characterized as an ATP non-competitive inhibitor CID755673 showed *in vitro* selectivity over 48 kinases at 10 uM, including several related kinases - PKCα, PKCβ, PKCδ, and CaMKIIα (Figure 4). Optimization of CID755673 through structural-activity relationship (SAR) resulted in the derivation of its benzoxoloazepinolone core, which led to a series of novel analogs. In a hit-to-lead initiative, KB-Nb142-70 represented the lead compound that exhibited an improved potency of 28 nM and 2.2 uM in enzymatic and cell-based assays, respectively (Figure 3)[43]. Biological evaluation of CID755673, Kb-NB142-70, and their derivatives demonstrated significant reduction in prostate cancer cell proliferation, migration, and invasion[42, 43]. Small molecule inhibition phenocopied siRNA-induced PKD knockdown; therefore, the study showed that pharmacological perturbation of PKD could suppress cancer-

associated biological responses. However, Kb-NB142-70's pharmacokinetic profile indicated poor metabolic stability. Undergoing phase I and II metabolism, rapid oxidation and glucuronidation of Kb-NB142-70 resulted in a plasma half-life of 6 minutes[44]. In order to abrogate these enzymatic modifications and improve its pharmacokinetic profile, the derivation of Kb-NB142-70 led to KMG-NB4-23, which contained an electron deficient methoxypyrimidine (Figure 3). KMG-Nb4-23 exhibited a relatively similar IC_{50} of 124 nM; however, due to poor aqueous solubility (less than 0.4 mg/mL), KMG-NB4-23 was not evaluated *in vivo*[45]. Although CID755673 and Kb-NB142-70 are not being pursued as therapeutic agents, they remain valuable compounds for probing PKD-regulated signaling events and biological activities *in vitro* and in cells.

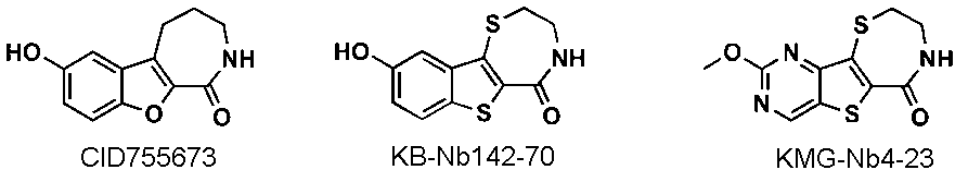

Figure 3. ATP non-competitive PKD small molecule inhibitors

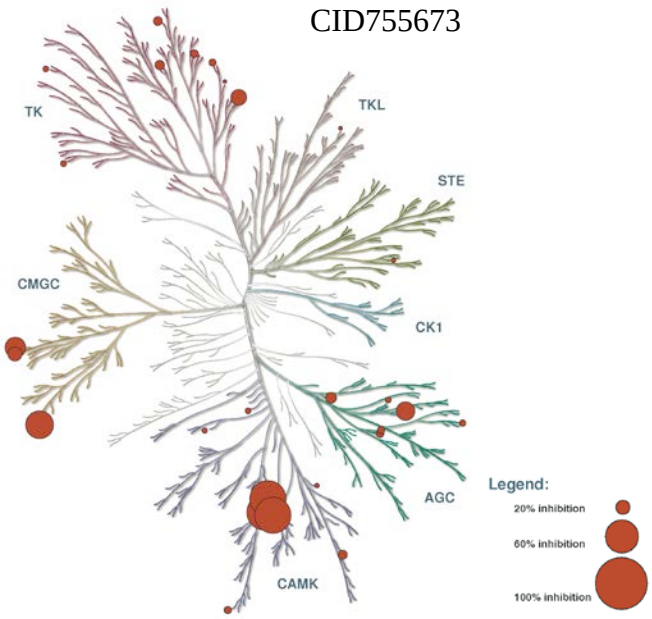

Figure 4. CID755673 Kinome Screen

In addition to CID755673 and its analogs, Novartis developed a series of ATP-competitive PKD inhibitors following an extensive HTS campaign and subsequent optimization through SAR analysis. Their lead naphthyridinylpyridinamine PKD inhibitor (NPKDi, Figure 5) targeted PKD at subnanomolar concentrations, having an impressive IC_{50} of 1 nM[46]. Investigating PKD associated-HDAC5 nuclear export in cardiomyocytes, NPKDi was able to abrogate PKD autophosphorylation and reduced PMA-stimulated phosphorylation of HDAC5 in isolated peripheral blood mononuclear cells (PBMC) from NPKDi-treated Dahl salt-sensitive (DSS) rats[46]. However, NPKDi showed poor selectivity. Out of a panel of 200 kinases, NPKDi potently targeted CaMKIIδ, GSKα/β, p38δ, MARK1/2 kinase at 1 μM (Figure 6)[47]. This limitation made it challenging to assess NPKDi's pharmacological inhibition of PKD in cardiac hypotrophy. Thus, an effort to find a more selective PKD inhibitor was pursued. The development of an ATP-competitive amidobipyridyl PKD inhibitor was reported to blunt *in vitro*

PKD1 activation at 1 nM (BPKDi, Figure 5). BPKDi also reduced HDAC phosphorylation in cell-based assays and provided improved selectivity over NPKDi off-target kinases at 1 uM (Figure 6)[47]. However, BPKDi failed to reduce pressure-overload-induced cardiac hypertrophy in both DSS and aortic-banded rats. This contradicts previous results, which revealed genetic knockout of PKD1 relieved pressure-overload-induced cardiac hypertrophy[48]. This may suggest pharmacological inhibition of PKD1 activity may not confer the same phenotypic response as PKD1 knockout. In general, discrepancies between genetic and pharmacological-based studies have been documented; although, in this case, further investigation is required to probe this variance[49]. Nonetheless, Novartis reported the first *in vivo* PKD targeted inhibitor that potently inhibited PKD activation and reduced HDAC5 nuclear export. Furthermore, in their animal study, NPKDi was administered orally up to 50 mg/kg/day with no apparent toxicity. However, due to poor solubility and negligible bioavailability, BPKDi required subcutaneous administration at up to 5 mg/kg/day. In order for these inhibitors to provide clinical value, modifications to improve their PK/PD and ADME profiles will be necessary.

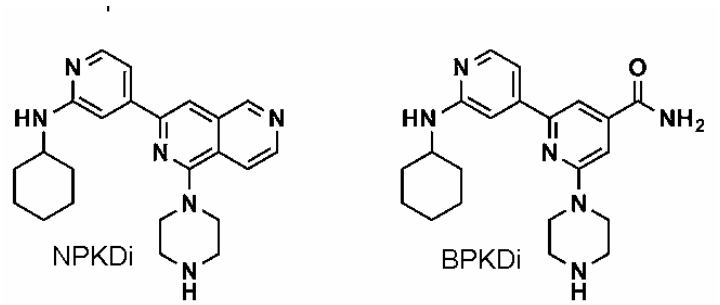

Figure 5. NPKDi and BPKDi chemical structure

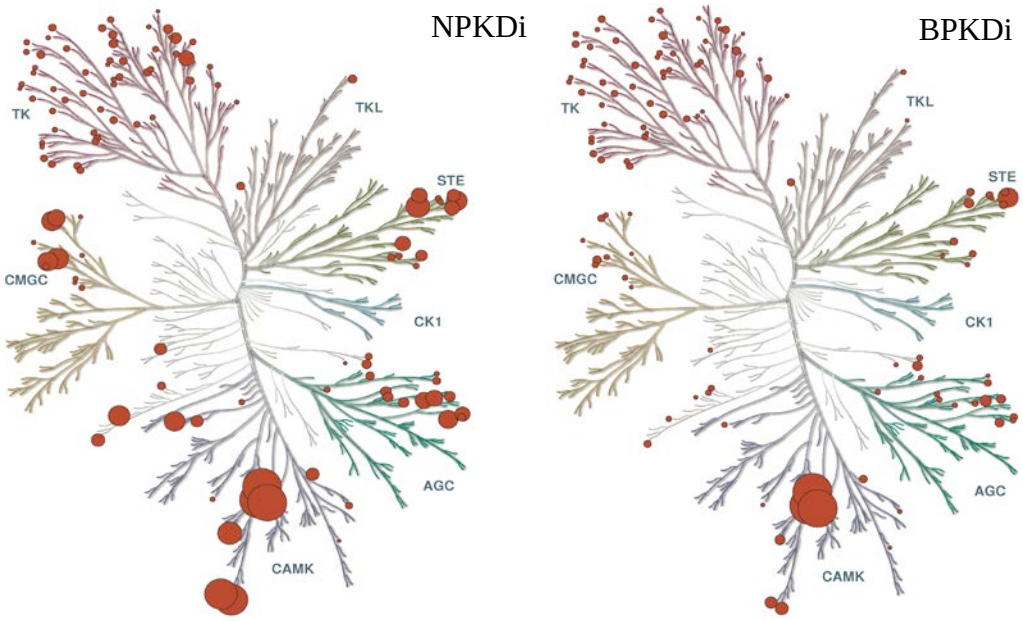

Figure 6. NPKDi and BPKDi Kinome Screen

Cancer Research Technology drug discovery program was next to report CRT0066051 and CRT0066101, an aminopyridine phenyl- and an aminopyrimidine phenol-based ATP-competitive PKD inhibitor, respectively (Figure 7). The two CRT independent series targeted PKD1 at subnanomolar concentrations (0.4 and 0.7 nM, respectively) and portrayed submicromolar activity in cell base assays. Moreover, in a limited kinome screen of 36 kinases, CRT0066051 was shown to be *very* selective for PKD compared to CRT006610, which has limited off target effects, inhibiting CDK2, IKKα, PRK2, and Rsk1 at 1 uM (Figure 8). Biological evaluation of human umbilical vein endothelial cells (HUVEC) showed treatment with CRT0066051 reduced VEGF-induced endothelial cell proliferation, migration, and tubulogenesis, suggesting a role of PKD in angiogenesis[50]. This study revealed CRT0066051 efficacy in cells; however, its ADMET properties were not determined and therefore its *in vivo* profile is currently unknown. Investigating PKD in a pancreatic cancer mouse xenograft model,

CRT0066101 significantly reduced tumor progression by abrogating PKD activation, stunting cell proliferation, and inducing apoptosis *in vivo*[51]. Importantly, CRT0066101 showed excellent oral bioavailability and no toxicity was observed at an oral dosage of 80 mg/kg/day[51]. Currently, CRT0066101 is the most promising PKD small molecule inhibitor; however, further investigations will be required before CRT0066101 can advance toward a clinical setting.

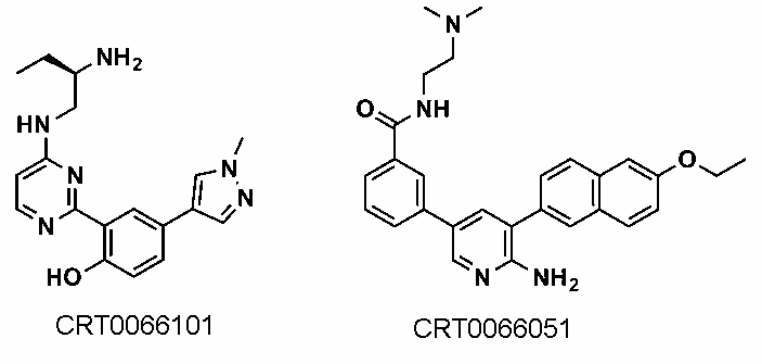

Figure 7. CRT0066101 and CRT0066051 chemical structure

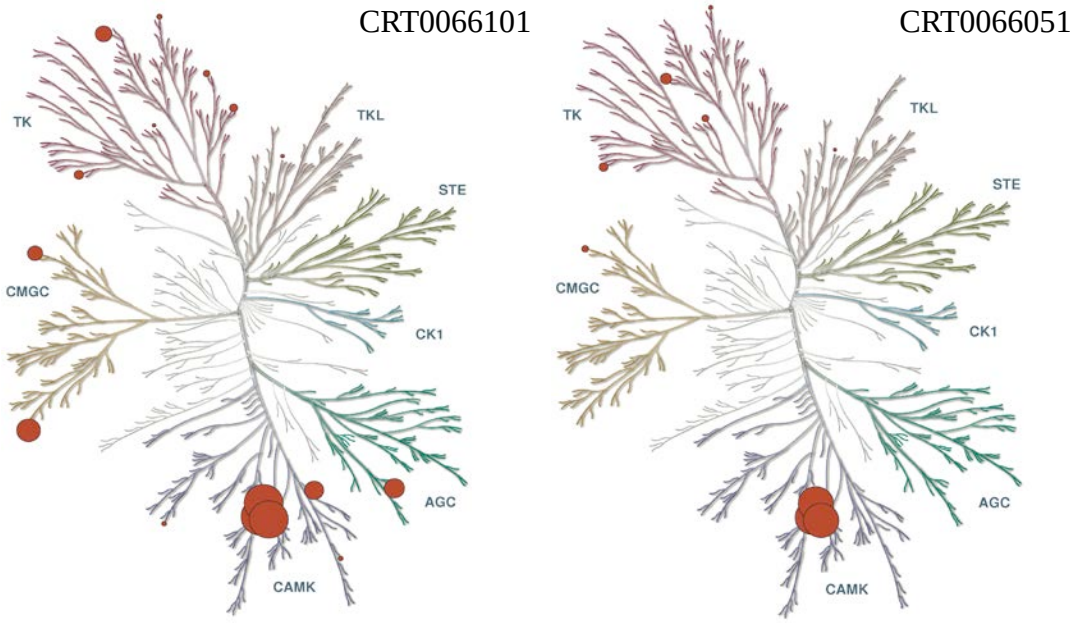

Figure 8. CRT0066101 and CRT0066051 Kinome Screen

In addition to the development of inhibitors that selectively block PKD activity, several dual PKD inhibitors were identified. These new PKD inhibitory scaffolds are the result of small-scale kinase-targeted library screens. Among them, Roche 139, a 4-azaindole scaffold from Hoffmann-La Roche, Inc. was found to potently inhibit PKD at 16.8 nM (Figure 9.)[52]. Although it is selective against PKC and CaMK family kinases, investigations into known 4-azaindole kinase inhibitors revealed Roche 139 effectively targets p38α MAP kinase at low nanomolar concentrations. Therefore, future drug discovery studies may provide Roche 139 an opportunity as a multi-targeted protein kinase inhibitor. The most recent PKD inhibitor, SD208 contains a pteridine core and targets PKD at low submicromolar concentrations (Figure 9). Originally employed as a potent TGFβ receptor I inhibitor, recent studies indicated SD208 potently inhibits PKD at similar concentrations, therefore SD208 can be employed as a dual PKD/TGFβRI inhibitor. Moreover, in a prostate cancer tumor xenograft model mice treated with SD208 showed a marked decrease in tumor growth. Thus, SD-208 represents a novel PKD inhibitory chemotype with *in vivo* efficacy that could potentially be further developed into a cancer therapeutic.

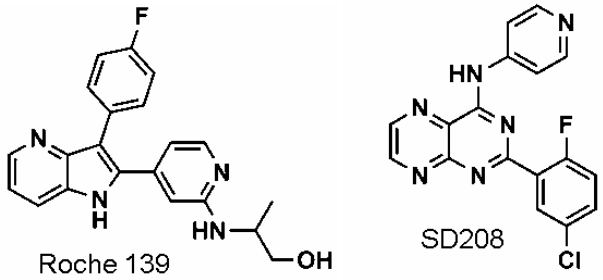

Figure 9. Roche139 and SD208 chemical structure

1.2 KINASE DOMAIN

1.2.1 Kinase Structure

Protein kinases contain a catalytic domain that is composed of a conserved globular structure featuring two lobes, N- and C-terminal lobe (Figure 10A). The N-terminal lobe is relatively smaller in size and primarily consists of a β-sheet and a single α-helix, which is known as the αC-helix. The C-terminal lobe is considerably larger and mostly alpha helical. A peptide chain called the hinge connects this bi-lobed system and establishes an intervening cleft recognized as the catalytic core. ATP binds within this region and forms critical hydrogen bonds between the nitrogen atoms of the adenine ring and the peptide backbone of the hinge (Figure 10B). This aids in positioning the purine moiety in a favorable environment, forming van der Waals interactions with nearby nonpolar aliphatic residues. Additional interactions critical for ATP binding rely on several conserved residues distinguished in the kinase active conformation. The activation of protein kinases and the subsequent binding of ATP is regulated by the activation loop, a short segment located in the C-terminal lobe near the ATP binding site. The activation loop begins with a conserved DFG motif, which plays an important role in defining the kinase's active conformation. In an activated state, the aspartate of the DFG motif chelates a magnesium ion, thereby stabilizing the alpha and gamma phosphate groups of ATP. Additional residues in the N-terminal lobe further support the phosphate groups and assist in optimally positioning ATP for catalysis. A conserved glutamate found in the αC-helix coordinates with a lysine in the β3 strand, which enables lysine to associate with the α- and β-phosphate groups of ATP. Further interactions occur between the active kinase domain and ATP; however, loss of the conserved aspartate from DFG or lysine confers a functionally incompetent kinase[53, 54].

A.

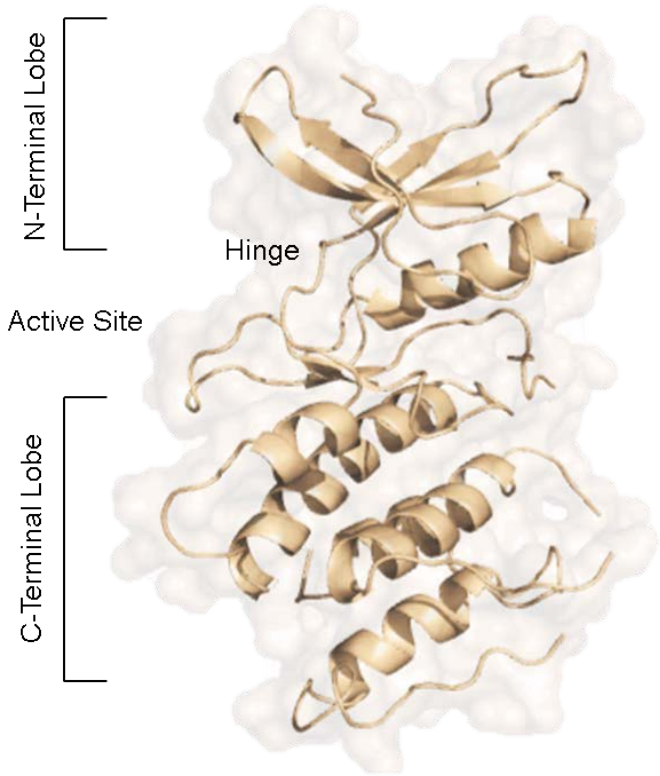

B.

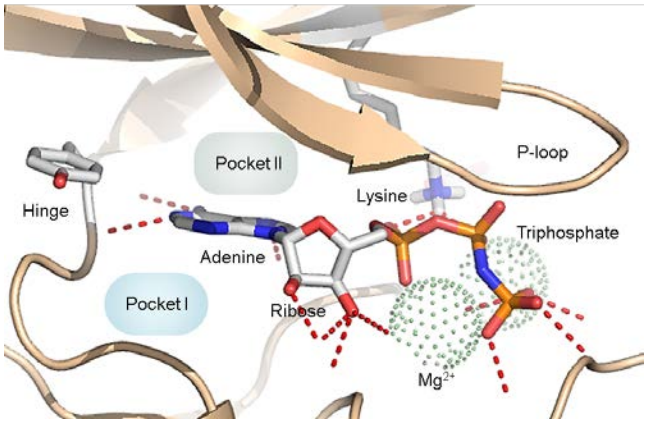

Figure 10. Kinase domain structure

A. Bi-lobed architecture. **B.** ATP bound in a kinase active site. (PDB:1O6L)

1.2.2 Small Molecule Kinase Inhibitors

The association of protein kinases in various diseases resulted in the pursuit of kinase inhibitors. To date, most kinase inhibitors compete with ATP binding, thereby, abrogating the kinase's catalytic function[55]. ATP-competitive inhibitors exhibit various heterocyclic scaffolds that can mimic the hydrogen bond formation of the adenine ring of ATP with residues at the hinge region. Type I inhibitors represents the majority of ATP-competitive inhibitors and target the kinase in its active conformation[56]. Therefore, type I inhibitors traditionally target regions near the ATP binding site and exploit distinct kinase properties, which contribute to their potency and selectivity[57]. A common place for exploitation is a solvent exposed hydrophobic pocket (pocket I) located at the hinge region near the entrance of the active site (Figure 11). An internal hydrophobic pocket (pocket II), which is partitioned by the gatekeeper residue, is also an area of exploitation[56]. In contrast, type II inhibitors recognize the inactive conformation. Due to the adopted DFG-out conformation associated in the kinases inactive state, type II inhibitors have additional exposure to an allosteric site neighboring the ATP binding site (Figure 11). Due to greater conformational heterogeneity of inactive protein kinases, it is suggested that type II inhibitors have the capability for improved kinase selectivity. However, allosteric inhibitors, which bind outside the ATP-binding site tend to exhibit the greatest kinase selectivity since they likely target regions unique to the kinase.

A.

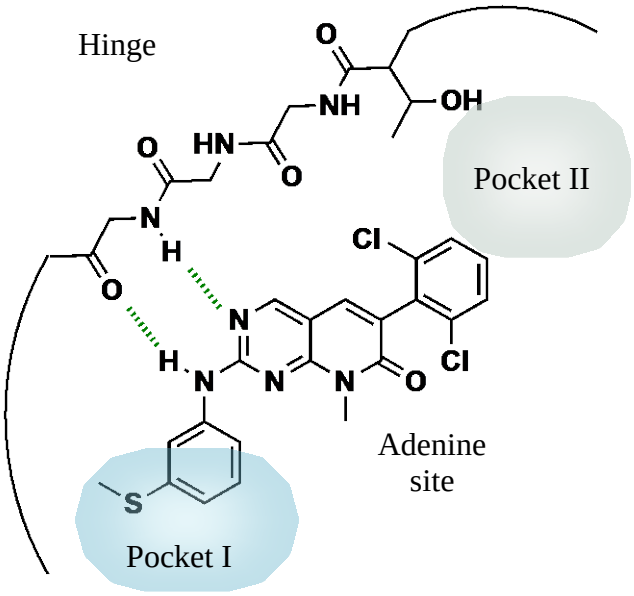

B.

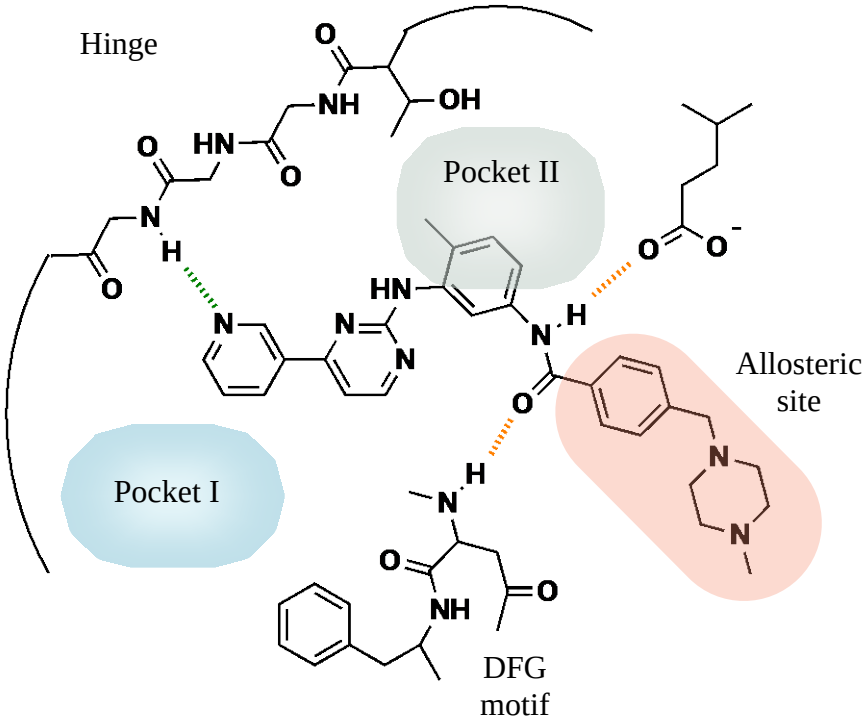

Figure 11. Small molecule kinase inhibitors bound in the active site

A. Type I ATP-competitive inhibitor **B.** Type II ATP-competitive inhibitor

2.0 MOLECULAR FEATURES ASSOCIATED WITH PKD SMALL MOLECULE BINDING

2.1 INTRODUCTION

The pursuit of PKD small molecule inhibitors has provided a diverse set of inhibitory scaffolds that show promising pharmacological and biological properties. However, the key chemical features associated with PKD inhibition are unknown. Access to structural information can greatly accelerate PKD drug discovery efforts and allow future initiatives to benefit from structure-based drug design. In the case of PKD, there is currently no crystal structure available, which makes rational design of potent and selective PKD inhibitors a considerable challenge. Therefore, through careful analysis of the chemical features of known PKD inhibitors and their respective SAR, we developed a PKD homology model to determine putative binding modes of PKD inhibitors within the kinase active site. This analysis alluded to structural determinants important for PKD inhibition and provided valuable structural details, which will aid in the future design of more potent and selective PKD inhibitors.

2.2 MATERIALS

2.2.1 Homology Model Generation

Currently, there is no crystallographic data for PKD; therefore, to investigate the structural features necessary for PKD small molecule inhibition, we developed a PKD homology model using the I-TASSER server. Submitting the primary amino acid sequence of PKD's kinase domain (residues 587 to 835), the I-TASSER performed a position-specific iterated BLAST (PSI-BLAST) to identify evolutionarily similar homologs. Aligning these proximal relatives assisted in the prediction of secondary structural motifs. The primary amino acid sequence in conjunction with the predicted secondary structures were employed to retrieve template proteins with similar folds from the Protein Data Bank (PDB) library using LOMETS threading, a locally installed meta-threading approach. The subsequent protein structures were selected as templates: 1QL6 (rabbit, phosphorylase kinase), 2BDW (c. elegans, calcium/calmodulin kinase II), 3MFR (human, calcium/calmodulin activated serine-threonine kinase), 2JAM (human, calcium/calmodulin-dependent protein kinase I G), and 2Y7J (human, phosphorylase kinase gamma 2). Following this threading procedure, the I-Tasser program split the templates into fragments based on template-sequence alignment and reassembled the fragments to create full length models. These resulting models were refined to their lowest energy state utilizing REMO and FG-MD programs, which optimized the C alpha backbone torsional angles, bond lengths, and side chain rotatmer orientations to generate fully refined, high quality predictive models of PKD's three-dimensional structure.

2.2.2 Docking Parameters

To perform docking calculations on PKD small molecule inhibitors, we employed the Surflex-Dock GeomX (SFXC) program using Sybyl-x 2.1 software. For each homology model of PKD's kinase domain all hydrogen atoms were present. The docking site, known as the Surflex-Dock Protomol, is the volumetric space in which inhibitors are evaluated. The protomol was configured to specifically target the ATP binding pocket and constructed using the following residues: Ala610, Lys612, Met659, Glu660, Lys661, Leu662, His663, Glu710, Leu713, Cys726. Additionally, the protomol was restricted to a threshold of 0.6 and a bloat of 3.0, which resulted in a sufficient pocket to conduct docking calculations. The SFXC program was instructed to evaluate an additional twenty starting conformations per molecule. Moreover, we introduced flexibility to protein atoms whose distance was less than 4 Å from the docked ligand. Ligands were prepared according to the Docking_Conformation protocol, which generate a SLN file of multiple samples of tautomers, stereoisomers, and conformers. The designed protomol as well as the ligand's SLN file was entered into SFXC program for docking analysis.

2.2.3 Homology Model Validation

Despite receiving high quality models from the I-TASSER server, there was a level of considerable uncertainty associated with the resulting predictive structures. Therefore, we assessed and validated models based on experimental findings. Docking calculations of literature reported PKD inhibitor NPKDi was performed using the Surflex-Dock GeomX (SFXC) program under the previously described parameters. The binding modes as well as key amino acid interactions were compared to that presented in literature. Specifically, models were evaluated

according to their ability to produce high docking scores, resulting from interactions with hinge residue Leu662, conserved catalytic residue Lys612, and sugar pocket residue Glu710 (Figure 22).

2.2.4 Docking of PKD Small Molecules Inhibitors

Employing our PKD homology model, we rationally determined putative binding modes for PKD small molecule inhibitors. Docking calculations were performed as previously described. Binding modes were initially evaluated according to their compliance with the characteristics appropriate for type I ATP-competitive inhibitors. The remaining binding modes were assessed according to their agreement with their respective experimentally derived structural activity relationship analysis. The most rational putative binding mode for each inhibitor evaluated was selected.

2.3 RESULTS AND DISCUSSION

A.

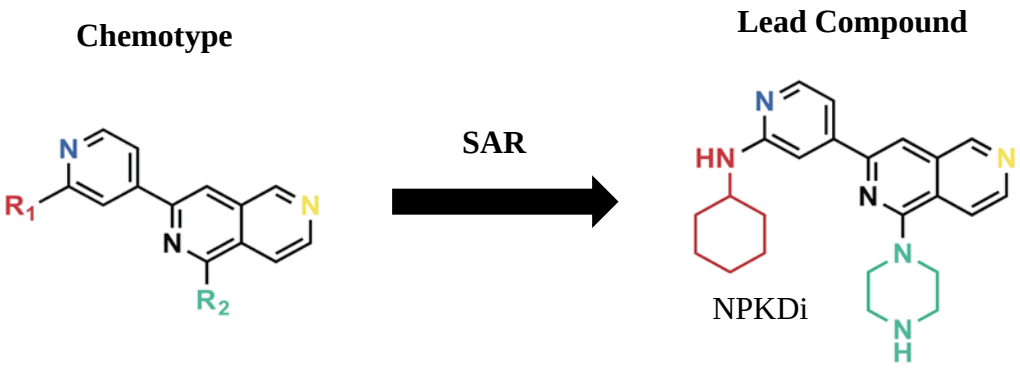

B.

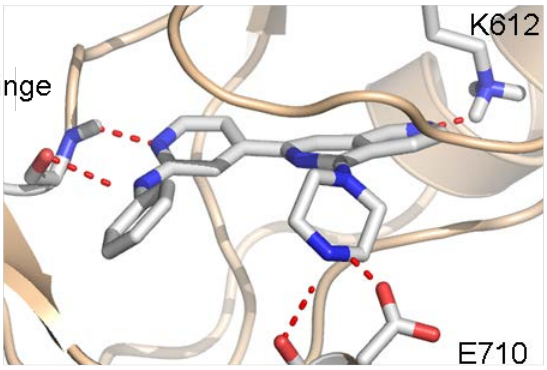

Figure 12. Structural investigation of NPKDi

A. SAR evaluation **B.** Molecular modeling

Novartis' investigation of the 2,6-naphthyridine scaffold revealed distinct chemical features associated with PKD inhibition. Initial functionalization of the naphthyridine core (black) led to the addition of 1-piperazine (**R_1**= H, **R_2**= piperazine: green), which resulted in more than a 200-fold increase in PKD selectivity over PKCα (Figure 12A). In addition, introduction of cyclohexylamine (**R_1**=cyclohexylamine: red, **R_2**= piperazine: green) at the 2-pyridine position afforded subnanomolar activity (0.6 nM) against PKD and remarkable

selectivity over PKC isoforms PKCα and PKCδ. Molecular modeling of NPKDi suggested a putative binding mode within the active site and provided rationale for PKD inhibition (Figure 12B). The nitrogens from the cyclohexylamine (red) and pyridine (blue) of NPKDi form two hydrogen bonds with the peptide backbone of Leu662 at the hinge region. The cyclohexyl group is positioned in pocket I and the piperazine was found in the ribose sugar region where it can form a salt bridge with Glu710. The 6-nitrogen (yellow) from the naphthyridine core generated a hydrogen bond with the positively charged side chain of the catalytic residue Lys612. SAR analysis indicates that other nonpolar alkylamine substituents in the $\mathbf{R_1}$ position were well tolerated. Additionally, it confirmed the basic nitrogen in the piperazine ring (green) as well as the nitrogen in the naphthyridine core (yellow) is necessary for inhibition. Loss of either one of these chemical components resulted in decreased potency. Thus, these findings offer great insight into PKD's active site and suggest important chemical characteristics for PKD inhibition.

A.

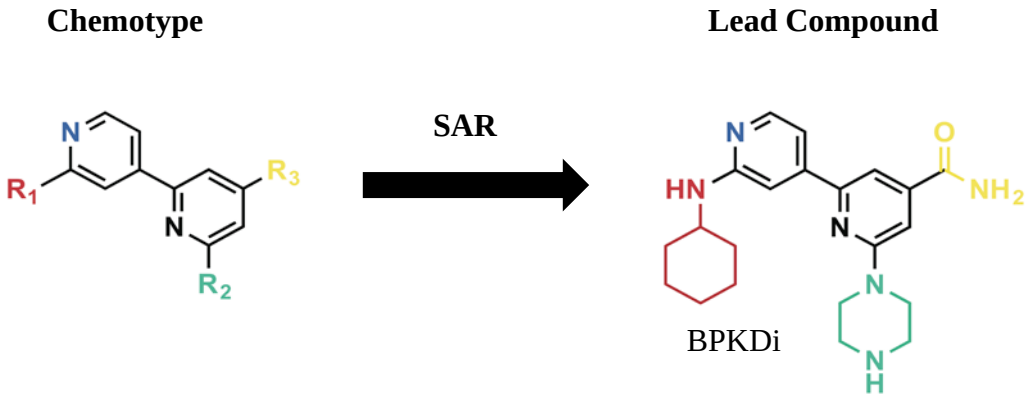

B.

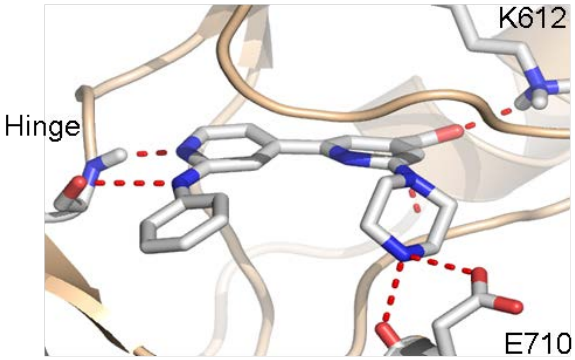

Figure 13. Structural investigation of BPKDi

A. SAR evaluation **B.** Molecular modeling

Following the structural guide established from the development of NPKDi, the design of an amidobipyridyl PKD inhibitor maintained similar chemical features. BPKDi retained the cyclohexylamine (red) and piperazine (green) functionality (Figure 13A). Since the amidobipyridyl chemotype (black) relinquished a fused ring system, $\mathbf{R_3}$ substituents with hydrogen bond capabilities with Lys612 were investigated. Introduction of a primary amide group (yellow) showed low nanomolar potency (1 nM). Pyrazole derivatives were also found to be equally as potent. Moreover, BPKDi has a marked improvement in its selectivity profile (Figure 6). Since the chemical structures of BPKDi and NPKDi are similar and their PKD

inhibitory activities are comparable, this differential in selectivity is rather significant. As shown in Figure 13B, molecular modeling results suggested that the primary amide forms additional interactions with residues positioned in pocket II, which we believe may be conducive for its improved PKD selectivity. Further investigation into selectivity is required. These findings reaffirm the chemical characteristics associated with NPKDi inhibition and suggested possible trends in targeting PKD.

A.

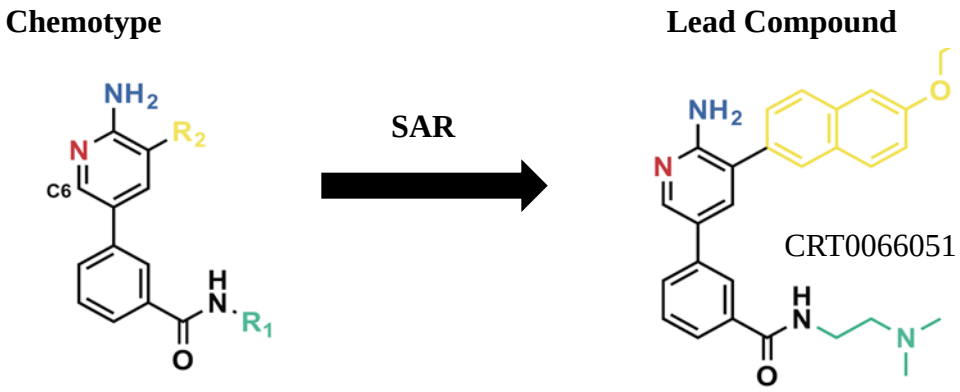

B.

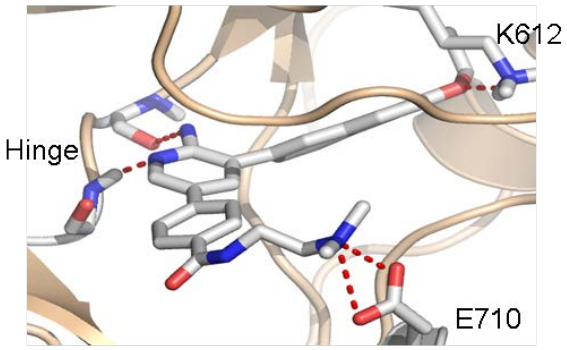

Figure 14. Structural investigation of CRT0066051

A. SAR evaluation **B.** Molecular modeling

In contrast to BPKDi, CRT0066051 has an amino pyridine core with 6-ethoxy-2-naphthyl and N,N-dimethylaminoethylbenzamido substituents. Studies into this compound revealed the

value of the 2-aminopyridine, which parallels the functionality of adenine of ATP. Removal of the exocyclic amino group (blue) or changing its position from C-2 to C-6 resulted in decreased potency (Figure 14A). Additionally, alkylation of exocyclic amine was shown to be detrimental to PKD activity. As illustrated in Figure 14B, molecular modeling suggested this functionality forms classical hydrogen bonds with the peptide backbone of residues at the hinge region, thereby positioning the inhibitor within the ATP binding site. Therefore, alkyl functionalization of the exocylic amine would potentially disrupt hydrogen-bonding interactions at the hinge or clash with the gatekeeper residue, thereby interfering with inhibitor binding. The N,N-dimethylaminoethylacetamide side chain was also found to be important for PKD inhibition. Upon inspection of $\mathbf{R_1}$ substituents, two carbon atoms are preferred for the amino alkyl chain (green) and loss of the terminal amino group resulted in an inactive compound, which makes this functionality critical for inhibition. Molecular modeling suggested the charged terminal amino group forms a salt bridge with Glu710, likening both Novartis' compounds. Additionally, the oxygen associated with the 6-ethoxy-2-naphthyl substituent (yellow) is positioned to form a hydrogen bond with Lys612. The 6-ethoxy group may extend into Pocket II, which could contribute to CRT0066051's excellent selectivity (Figure 8). Also, SAR analysis investigating $\mathbf{R_2}$ substitutions revealed functionality with hydrogen bond capabilities was tolerated and important for reduced enzymatic activity. Evaluation of CRT0066051 illustrated conserved interactions between PKD inhibitors and PKD's active site, suggesting possible trends in PKD inhibition.

A.

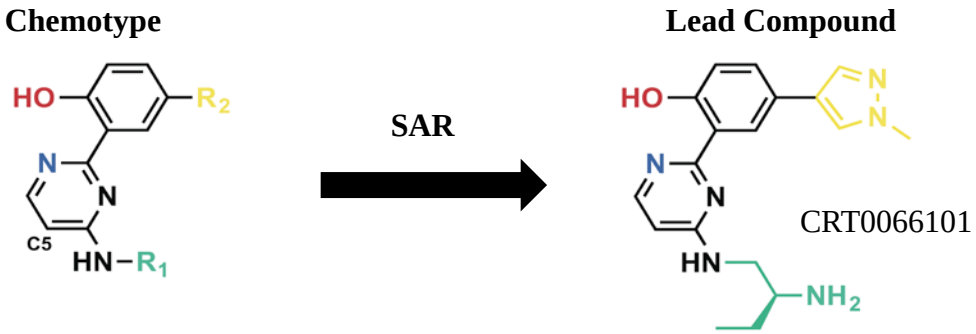

B.

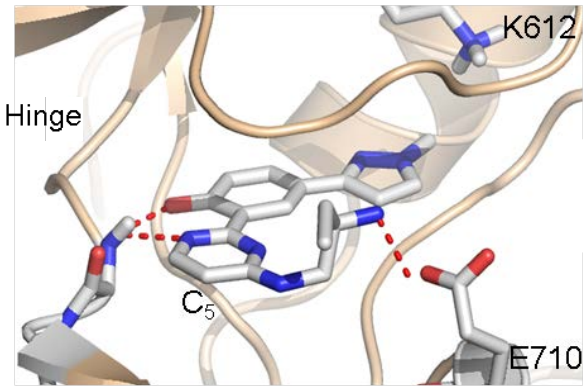

Figure 15. Structural investigation of CRT0066101

A. SAR evaluation **B.** Molecular modeling

CRT0066101 represents a novel chemotype, exhibiting an aminopyrimidine scaffold. Exploration of the $\mathbf{R_1}$ amino alkyl substituents found that the aminoethyl (green) was preferred over longer alkyl chains (Figure 15A). Small substituents alpha to the terminal amine was tolerated and helped improve potency as well as cell permeability. Additionally, like CRT0066051, the terminal amine was determined essential for PKD inhibition and our model showed it forms favorable interactions with Glu710. Investigations into the phenyl ring concluded the phenolic hydroxyl (red) is essential for inhibition. Additionally, evaluation of the pyrimidine concluded the nitrogen (blue) at the 1-position was also required (Figure 15B).

Molecular modeling revealed the oxygen (red) from the phenolic hydroxyl and the 1-nitrogen (blue) from the pyrimidine establish a hydrogen bond clamp with the peptide backbone at the hinge. Therefore, this proposed orientation of the pyrimidine would suggest the tolerance of C-5 substituents positioned into pocket I. Indeed SAR analysis confirmed that various derivations (e.g., methyl, phenyl, 4-pyrazole) at C-5 were well tolerated. Further exploration into the phenolic ring revealed that electron withdrawing $\mathbf{R_2}$ substituents para to the phenolic hydroxyl group was also tolerated. However, substitution at this position had marginal affect on potency, which implied no additional interactions are formed. In general, CRT0066101 is comparably more consolidated within PKD's active site; however, it distinctly exploits common features associated with PKD inhibition.

A.

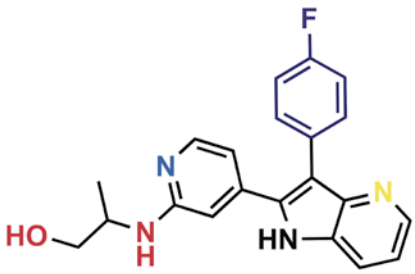

B.

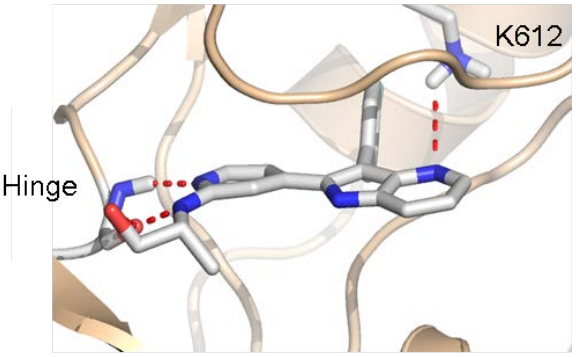

Figure 16. Structural investigation of Roche 139

A. Distinct chemical features **B.** Molecular modeling

Although early in development, we applied our understanding of PKD inhibition and rationalized putative binding modes for novel PKD inhibitors Roche 139 and SD208, suggesting potentially important interactions associated with their binding. Roche 139 has a 1H-pyrrolo[3,2-b]pyridine scaffold with 4-fluorphenyl and 2-alkylaminopyridyl substituents (Figure 16A). Investigation into this scaffold revealed a known 4-azaindole kinase inhibitor, **9** (as labeled in paper), which portrays similar chemical characteristics to Roche139 (Figure 23A). **9** is well characterized and has been co-crystalized with p38 MAP kinase. Applying our PKD analysis we deduced rational features associated with Roche 139 inhibition, which was supported by the co-crystal structure of **9**. As illustrated in Figure 16B, both nitrogens from the amino pyridine (red and blue) as well the oxygen (red) from the propan-1-ol side chain formed optimal hydrogen bonds with the peptide backbone of residues at the hinge region. Additionally, the 4-fluorophenyl substituent (purple) extends into pocket II and the nitrogen from the fused pyridine (yellow) formed a potentially critical hydrogen bond with the charged sided chain of Lys612. Both of these inhibitory characteristics were also illustrated in the binding of **9** in p38 MAP kinase (Figure 23B). Roche139 contains similar chemical features with other PKD inhibitors; however, it wasn't shown to exploit a valuable interaction with Glu710. Future efforts should consider additional functionalization, which may improve Roche139's potency and selectivity.

A.

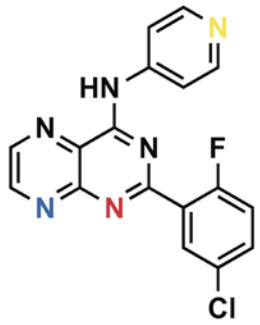

B.

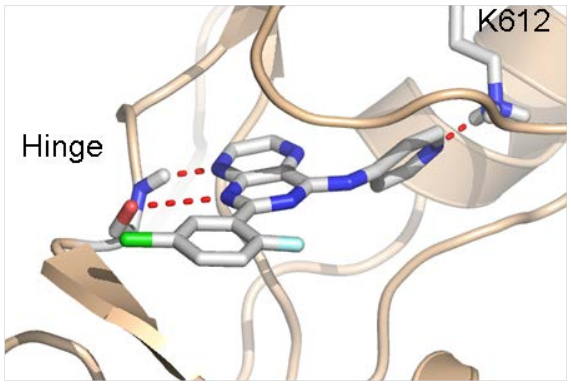

Figure 17. Structural investigation of SD208

A. Distinct chemical features **B.** Molecular modeling

In contrast to Roche 139, SD208 contains a pteridine core with 4-aminopyridyl and 5-chloro-2-fluorophenyl substituents (Figure 17A). Molecular modeling of SD208 revealed hydrogen-bonding interactions between the amino acids at the hinge region and its nitrogens in the pteridine core (red and blue). Additionally, SD208 may also form a potentially critical hydrogen bond with the nitrogen from the 4-aminopyridine (yellow) and the charged side chain of Lys612 (Figure 17B). The limited SAR analysis conducted for SD208 supported the notion that the nitrogen from the 4-aminopyridine acts as a valuable hydrogen bond acceptor. Ablation

of this bond revealed a marked decrease in PKD1 inhibition. Interpreting this putative binding mode, it's possible that additional medicinal chemistry efforts could functionalize select positions of SD208 to take advantage of Glu710 and interactions within pocket II. This may enhance potency and improve SD208's selectivity for PKD.

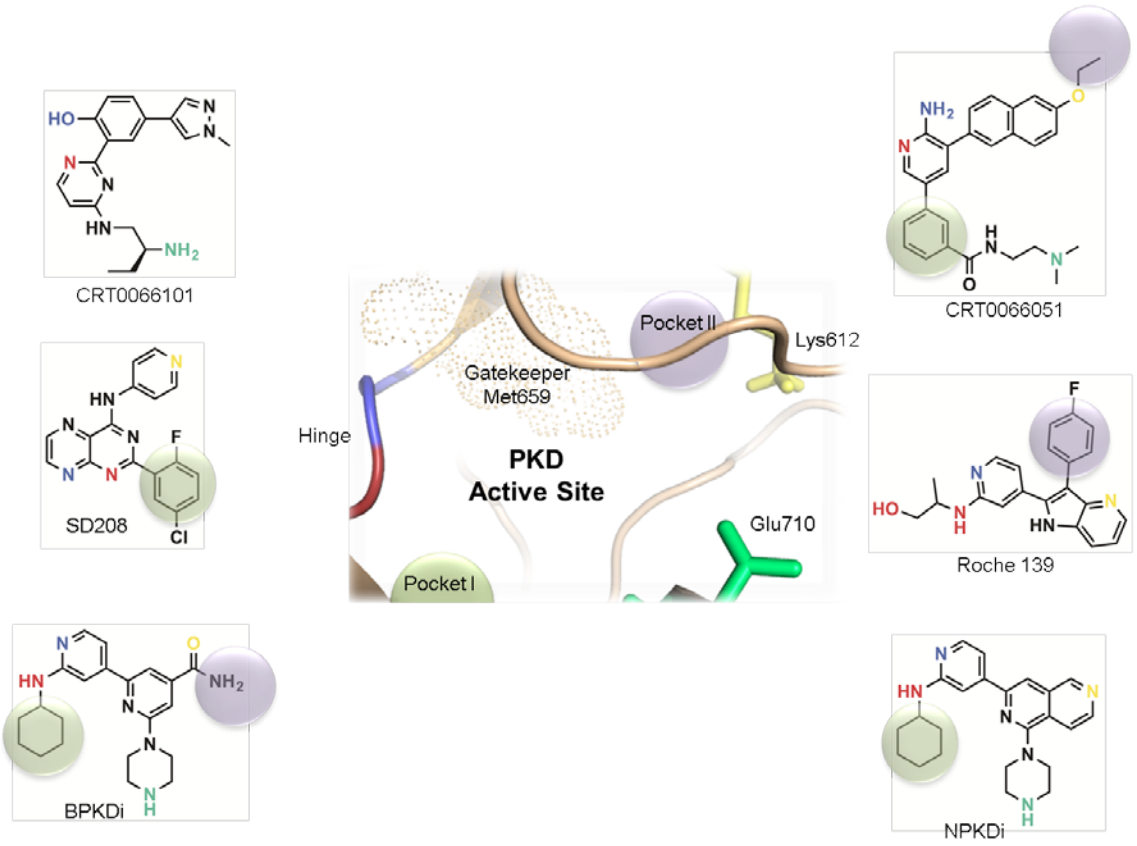

Figure 18. Trends in putative binding modes of PKD small molecule inhibitors

Molecular modeling and SAR analysis of PKD small molecule inhibitors highlighted key chemical elements and unique structural features required for PKD inhibition (Figure 18). Common among ATP-competitive inhibitors, a core heterocyclic scaffold was necessary to form hydrogen bonds at the hinge region in a similar fashion to adenine of ATP. An orthogonal substituent or linker that traverses the active site positioned an additional hydrogen bond acceptor to interact with the charged side chain of Lys612. This substituent or linker could be

relatively flexible (e.g., BPKDi) or rigid (e.g., the fused aromatic ring system of NPKDi or CRT0066051); however, it carefully accommodated PKD's considerably large gatekeeper residue, Met659. Additionally, a functional moiety (typically a basic amino group) capable of developing a critical salt bridge with Glu710 was shown to be important for added affinity. Thus, this interaction can be generated by appropriately functionalizing the core heterocyclic scaffold (e.g., CRT0066101 and CRT0066051) or the traversing substituent (e.g., NPKDi and BPKDi). Exploiting the two hydrophobic pockets may improve improve potency and selectivity. For PKD, pocket I is likely solvent exposed and can tolerate both polar and non-polar groups. Due to the size of the sterically cumbersome gatekeeper residue, introducing favorable interactions within pocket II may be challenging. However, analyzing the selectivity profile of BPKDi and CRT0066051, we believe further functionalization in pocket II may dramatically reduce kinase off-target effects. Based on SAR analysis, it appeared small substituents are well tolerated. Further exploitation of pocket II could provide new information and may result in more selective PKD inhibitors. Future drug discovery efforts should look to take advantage of all the required chemical features to develop a more potent and selective PKD inhibitor.

3.0 BIOCHEMICAL INVESTIGATIONS INTO PKD SMALL MOLECULE INHIBITON

3.1 INTRODUCTION

Most kinase inhibitors target the kinase active site and compete with ATP binding, thereby, abrogating the kinase's catalytic function[55]. These ATP-competitive inhibitors contain various heterocyclic scaffolds that can mimic the hydrogen bond formation of the adenine ring of ATP with residues at the hinge region[56]. Type I inhibitors represents the majority of ATP-competitive inhibitors and target the kinase in its active conformation. Therefore, type I inhibitors traditionally target regions near the ATP binding site and exploit distinct kinase properties, contributing to their potency and selectivity[57]. A common place for exploitation is a solvent exposed hydrophobic pocket (pocket I) located at the hinge region near the entrance of the active site. This area can contain various amino acids that are uniquely positioned, offering heterogeneity among protein kinases. Kinase inhibitors that exploit this region position both polar and non-polar functional groups in pocket I[56]. Also, another targeted region is hydrophobic pocket II. Pocket II neighbors the ATP binding site and is partitioned by the gatekeeper residue, which dictates the relative cavity size of pocket II and regulates inhibitor accessibility[58]. Protein kinases have varying gatekeeper residues. Many tyrosine kinases contain a threonine amino acid at this position, which is a relatively small gatekeeper residue with hydrogen bond capabilities,

making the exploitation of pocket II advantageous[59]. Therefore, it is common for tyrosine kinase inhibitors to have functional groups positioned in this region. On the other hand, most serine/threonine kinases, like PKD, contain a larger methionine residue, thereby, making it considerably more challenging to access pocket II. Drug discovery efforts look to take advantage of these kinase-specific features, thus, having a structural understanding can provide the basis for rational drug design and improve kinase/inhibitor interactions.

It has been well reported that type I ATP-competitive inhibitors are affected by mutations in the ATP binding region. In a recent study investigating inhibitor resistance in protein kinases, investigators found point mutations at two specific positions within the ATP active site that reduced inhibitor sensitivity[60]. Specifically, select mutations of the gatekeeper residue or a downstream glycine residue found on the hinge loop near pocket I disrupted inhibitor binding. Since there is currently no experimental data suggesting the binding modes of PKD small molecule inhibitors, we postulate that mutations at these two regions to larger, more sterically cumbersome amino acids would selectively interfere with inhibitor exploitation. PKD small molecule inhibitors offer a variety of diverse inhibitory scaffolds, so it is possible that these mutations could have varying effects. Therefore, we introduced individual amino acid substitutions at the gatekeeper and into the hinge region of PKD and evaluated inhibitor sensitivity.

3.2 MATERIALS AND METHODS

3.2.1 Antibodies for immunoblotting, kinase substrates, and inhibitors

The following antibodies were used for immunoblotting: rabbit anti-phosphoSer916 PKD1 (working dilution 1:2000; Millipore), mouse anti-flag (working dilution 1:2000), mouse anti-tubulin (working dilution 1:2500; Santa Cruz Biotechnology). CRT0066101 was a kind gift from Cancer Research Technology.

3.2.2 Cell stimulation, inhibitor treatment, and cell lysis

HEK 293 cells were transfected with the plasmid containing the indicated Flag-PKD1-WT or Flag-PKD1-mutant using Lipofectamine 200 transfection reagent according to the manufacturer's suggestions. The cells transfected with indicated Flag-PKD1-WT and Flag-PKD1-mutant were deprived of serum for 18 hr. PKD inhibitor, CRT0066101, or the equivalent volume of DMSO as a control, was added to the cell culture medium 90 minutes prior to stimulation. The cells were then stimulated with 10 nM PMA for 20 minutes. Finally, treated HEK 293 cells were lysed in 50 mM Tris-HCl, pH 7.4, 150 mM NaCl, 1.5 mM $MgCl_2$, 10% glycerol, 1% Triton X-100, 5 mM EDTA, 20 μM Leupeptin, 1 mM phenylmethylsulfonyl fluoride (PMSF), 1 mM $NaVO_3$, and 10 mM NaF, and incubated on ice. Cell lysates went through three consecutive freeze-thaw cycles and centrifuged for 10 minutes at 13,000 rpm at 4 °C in an Eppendorph microcentrifuge. Protein amounts were measured with BCA Concentration Assay kit (Pierce) as specified by the manufacturer, and equivalent amounts of total protein of each cell lysate were analyzed by western blot.

3.2.3 Western blot analysis

Western blot analysis was carried out to analyze expression of various proteins. Equal amounts of protein were subjected to SDS-PAGE and subsequent electrotransfer to nitrocellulose membranes. Membranes were pre-blocked in 5% nonfat milk in Tris-buffered saline with 0.01% Tween-20 (TBS-T) and then incubated with primary antibodies in 5% BSA overnight at 4°C. Primary antibodies against pS916-PKD1, flag, and tubulin were used. Membranes were washed in TBS-T and then incubated for 1 h at room temperature with secondary anti-rabbit or anti-mouse antibodies conjugated to horseradish peroxidase (HRP, Bio-Rad). Detection of specific protein bands was facilitated by the enhanced chemiluminescence (ECL) Western blotting detection system (Amersham Biosciences). Densitometry analysis was performed using Image Lab from ChemiDoc MP System (Bio-Rad).

3.3 RESULTS AND DISCUSSION

A.

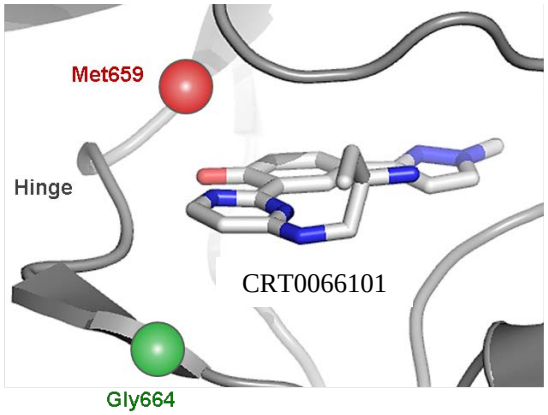

B.

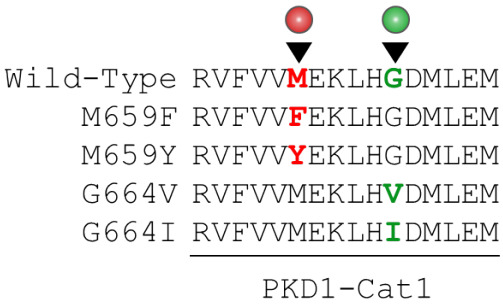

Figure 19. Structural basis for PKD1 active site mutations

A. Cartoon representation of the active site of a PKD1 kinase homology model bound to CRT0066101. Residues selected as candidates for mutation in this study are illustrated by spheres (red: gatekeeper residue, Met659; green: pocket I residue, Gly664). Molecular models were rendered with pymol (www.pymol.org). **B.** Sequence alignment of the hinge region of PKD kinase domain. The mutations highlighted are the gatekeeper residue M659 (red) and pocket I residue Gly664 (green).

Experimental evidence describing PKD small molecule inhibitor positioning within PKD's kinase domain is unknown. Therefore, to explore inhibitor binding and to investigate regions of kinase exploitation within PKD's active site, we independently generated select mutations and evaluated its effects on kinase sensitivity. Specifically, we conducted site-directed mutagenesis of PKD's gatekeeper residue, Met659, and hinge residue, Gly664, positioned at pocket I (Figure. 19). We posited that mutating these residues to larger, more sterically cumbersome amino acids would obstruct inhibitor binding and thereby, desensitize PKD from pharmacological inhibition.

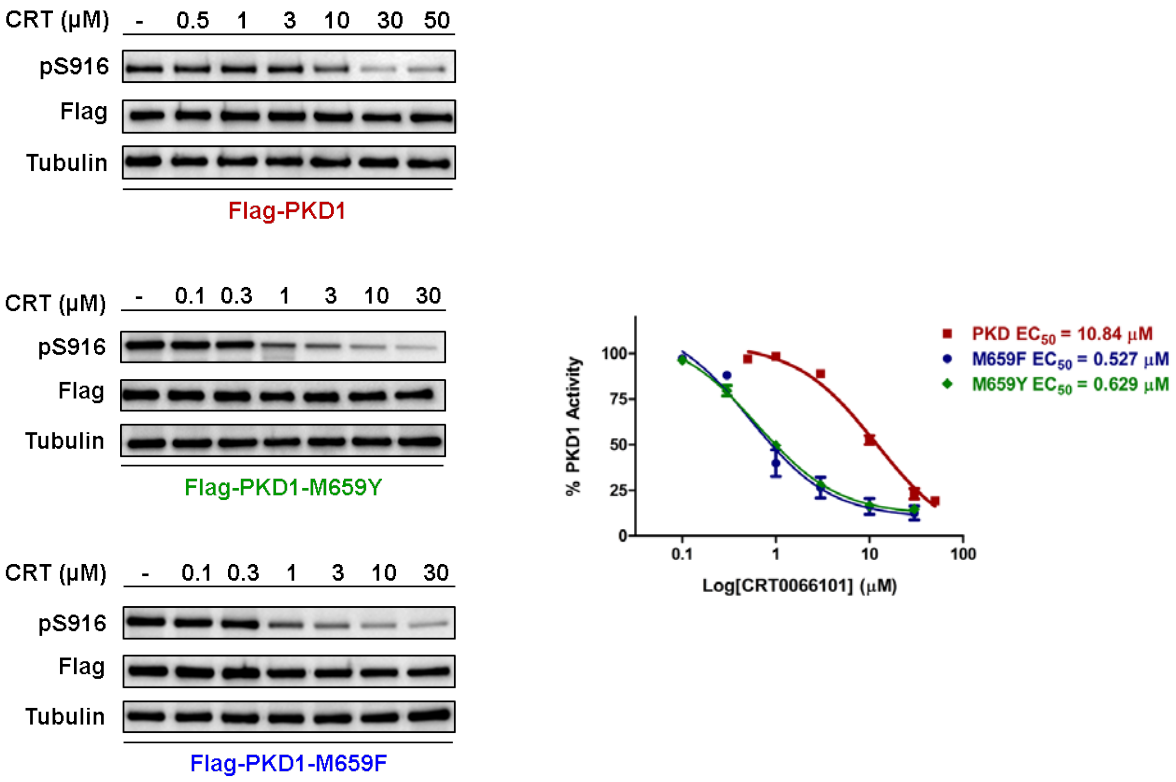

Figure 20. Cellular PKD1 mutant sensitivity to CRT0066101 treatment

HEK 293 cells transiently expressing Flag-PKD1-WT, Flag-PKD1-M659Y, and Flag-PKD1-M659Y were serum starved for 18 hours. Following, cells were treated with the indicated concentration of CRT0066101 for 90 minutes and subsequently induced with 10 nM of PMA. Cells were collected and lysed. Total cell lysate was analyzed by immunoblotting with anti-pSer916 PKD1-specific antibody for kinase activity, anti-flag antibody for transfection efficiency, and anti-tubulin for loading control. Densitometric quantification was performed using Image Lab (Bio-Rad) and the activity was normalized against the transfection efficiency and with the loading control.

To probe pocket II occupancy, we constructed Flag-PKD1-M659F and -M659Y mutants, which would reduce pocket II cavity size and limit the window for inhibitor exploitation. Expressing these mutants in HEK 293 cells in the presence of increasing concentrations of potent PKD small molecule inhibitor, CRT0066101, we anticipated reduced inhibitor activity compared to the treatment of Flag-PKD1-WT. Following western blot analysis of PKD1's activity according to PMA-induced PKD autophosphorylation at Ser916, we were surprised to observe an increase in CRT0066101 sensitivity. The cellular EC_{50} for Flag-PKD1-WT was determined to be 10.84 μM; however, for mutants Flag-PKD1-M659F and –M659Y their cellular EC_{50} was markedly reduced to 0.527 and 0.629 μM, respectively (Figure 20). These results suggest CRT0066101 does not occupy pocket II. More interestingly, M659F and M659Y amino acid substitutions enhanced inhibitor binding, which indicate these residues introduced a new chemical interaction and assisted with stabilizing CRT0066101 in PKD's active site. Both phenylalanine and tyrosine have aromatic amino acid side chains. It is possible that these residues allow for pi-pi stacking with an aromatic ring of CRT0066101. Based off of the rational

putative binding mode of CRT0066101 within our PKD kinase homology model, it is plausible that this non-covalent interaction occurs with the aromatic moiety of CRT006101's phenolic ring. It has been documented that pi-pi stacking can assist in drug binding, which in drug discovery, is commonly found through T-shaped or parallel-displaced interactions[61].

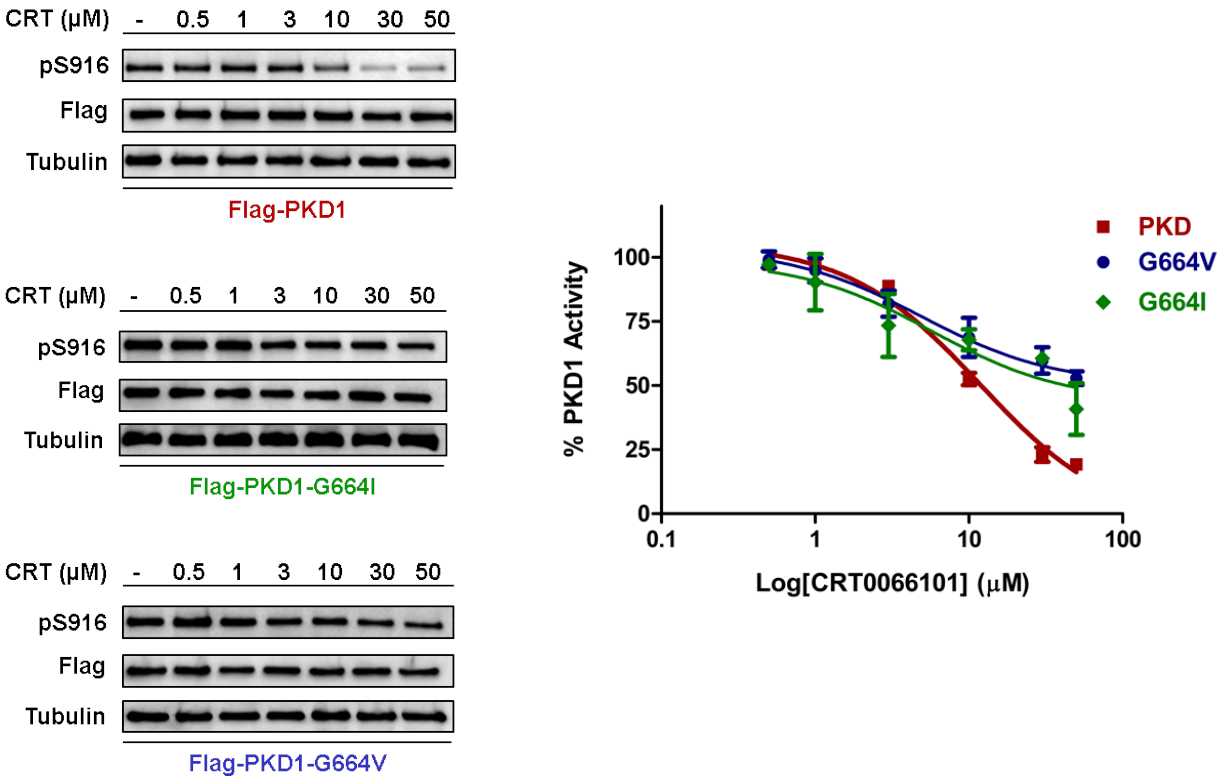

Figure 21. Cellular PKD1 mutant resistance to CRT0066101 treatment

HEK 293 cells transiently expressing Flag-PKD1-WT, Flag-PKD1-G664V, and Flag-PKD1-G664I were serum starved for 18 hours. Following, cells were treated with the indicated concentration of CRT0066101 for 90 minutes and subsequently induced with 10 nM of PMA. Cells were collected and lysed. Total cell lysate was analyzed by immunoblotting with anti-pSer916 PKD1-specific antibody for kinase activity, anti-flag

antibody for transfection efficiency, and anti-tubulin for loading control. Densitometric quantification was performed using Image Lab (Bio-Rad) and the activity was normalized against the transfection efficiency and with the loading control

Next, we investigated pocket I exploitation by making amino acid substitutions at Gly664. Pocket I is hydrophobic in nature; however, it is solvent exposed and can tolerate both polar and non-polar functional groups. Therefore, we constructed G664V and G664I mutants, which have hydrophobic, aliphatic side chains that would be positioned within PKD's active site. As previously described, we expressed Flag-PKD1-G664V and –G665I mutants in HEK 293 cells in the presence of increasing concentrations of CRT0066101. Comparing the kinase activity to Flag-PKD1-WT, western blot analysis of PKD1's activity according to PMA-induced PKD autophosphorylation at Ser916 indicated a decrease in CRT0066101 sensitivity (Figure 21). The cellular EC_{50} for Flag-PKD1-G664V and -G664I mutants was roughly 50 μM, which is an increase compared to Flag-PKD1-WT. This reduced sensitivity may suggest CRT0066101 exploits, to some degree, pocket I. Although, it is unclear how these pocket I mutations specifically affect CRT0066101 binding. At higher concentrations CRT0066101 no longer perturbs mutant PKD activity. This may indicate a change in CRT0066101's binding mode within PKD's active site, altering its mechanism of inhibition; however, in-vitro evaluations using recombinant protein is required to provide further insight.

The binding of PKD small molecule inhibitors within PKD's kinase domain is poorly understood. This investigation provided new insight into the positioning of CRT0066101 and described regions of exploitation within PKD's active site. In addition to improving our structural understanding of PKD inhibition, we indirectly developed a chemical genetic tool kit

to explore PKD within a biological system. Mutating the gatekeeper residue, Met659, to phenylalanine or tyrosine dramatically sensitized PKD to CRT0066101 inhibition. Conversely, mutating hinge residue, G664, to larger, more sterically cumbersome amino acids like valine or isoleucine conferred resistance. Therefore, these tools can be employed as a common strategy when evaluating PKD function using CRT0066101 pharmacological inhibition.

4.0 CONCLUSION AND FUTURE DIRECTION

The pursuit to abrogate PKD catalytic function has led to the discovery of a series of effective PKD small molecule inhibitors. However, these inhibitory scaffolds have not transitioned to the clinic and therefore, further drug discovery efforts are necessary to establish a potential drug candidate. The work presented in this document has provided insightful analysis of type I ATP-competitive PKD inhibitors and proposes putative binding modes that describe important chemical characteristics essential for PKD inhibition. Thus, future initiatives should employ rational drug design and incorporate the appropriate functionality necessary for enhanced potency and selectivity. We believe this improved structural understanding will facilitate in efficient development of PKD small molecule inhibitors, thereby, providing greater opportunity for the discovery of a novel PKD therapeutic agent.

APPENDIX A

MOLECULE MODELING

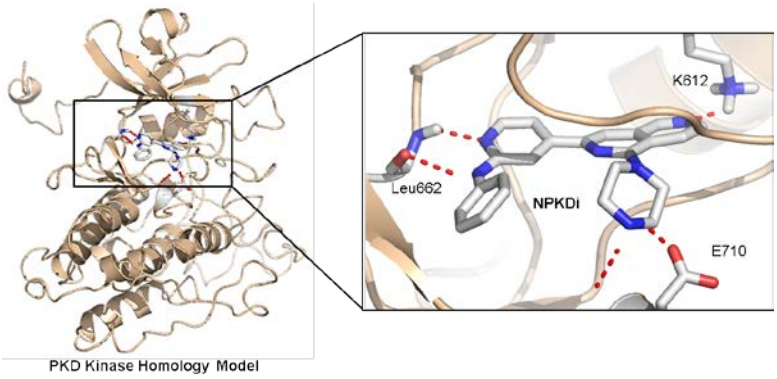

Figure 22. PKD kinase homology model validation

A.

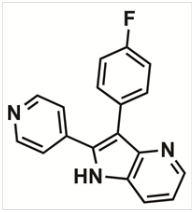

4-Azaindole, **9**

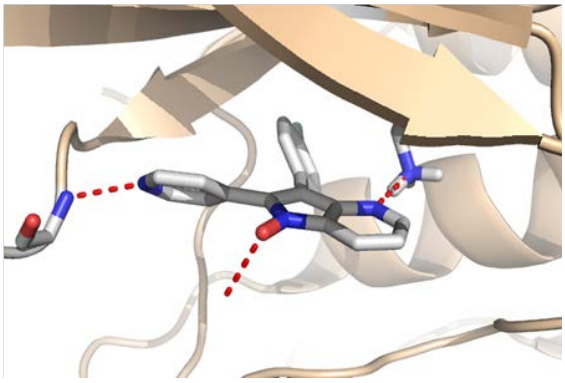

Figure 23. Structural investigation into 4-Azaindole kinase inhibitor

A. Chemical structure of 4-Azaindole, 9. **B.** 4-Azaindole, 9, bound to p38 MAP kinase

BIBLIOGRAPHY

1. Valverde, A.M., Sinnett-Smith, J., Van Lint, J. & Rozengurt, E. Molecular cloning and characterization of protein kinase D: a target for diacylglycerol and phorbol esters with a distinctive catalytic domain. *Proc Natl Acad Sci U S A* **91**, 8572-6 (1994).

2. Cohen, P. The origins of protein phosphorylation. *Nat Cell Biol* **4**, E127-30 (2002).

3. Johannes, F.J., Prestle, J., Eis, S., Oberhagemann, P. & Pfizenmaier, K. PKCu is a novel, atypical member of the protein kinase C family. *J Biol Chem* **269**, 6140-8 (1994).

4. Sturany, S. et al. Molecular cloning and characterization of the human protein kinase D2. A novel member of the protein kinase D family of serine threonine kinases. *J Biol Chem* **276**, 3310-8 (2001).

5. Hayashi, A., Seki, N., Hattori, A., Kozuma, S. & Saito, T. PKCnu, a new member of the protein kinase C family, composes a fourth subfamily with PKCmu. *Biochim Biophys Acta* **1450**, 99-106 (1999).

6. Rozengurt, E., Rey, O. & Waldron, R.T. Protein kinase D signaling. *J Biol Chem* **280**, 13205-8 (2005).

7. Matthews, S., Iglesias, T., Cantrell, D. & Rozengurt, E. Dynamic re-distribution of protein kinase D (PKD) as revealed by a GFP-PKD fusion protein: dissociation from PKD activation. *FEBS Lett* **457**, 515-21 (1999).

8. Cowell, C.F. et al. Mitochondrial diacylglycerol initiates protein-kinase D1-mediated ROS signaling. *J Cell Sci* **122**, 919-28 (2009).

9. Rey, O. & Rozengurt, E. Protein kinase D interacts with Golgi via its cysteine-rich domain. *Biochem Biophys Res Commun* **287**, 21-6 (2001).

10. Rebecchi, M.J. & Scarlata, S. Pleckstrin homology domains: a common fold with diverse functions. *Annu Rev Biophys Biomol Struct* **27**, 503-28 (1998).

11. Iglesias, T. & Rozengurt, E. Protein kinase D activation by deletion of its cysteine-rich motifs. *FEBS Lett* **454**, 53-6 (1999).

12. Iglesias, T. & Rozengurt, E. Protein kinase D activation by mutations within its pleckstrin homology domain. *J Biol Chem* **273**, 410-6 (1998).

13. Waldron, R.T. & Rozengurt, E. Protein kinase C phosphorylates protein kinase D activation loop Ser744 and Ser748 and releases autoinhibition by the pleckstrin homology domain. *J Biol Chem* **278**, 154-63 (2003).

14. Steinberg, S.F. Regulation of protein kinase D1 activity. *Mol Pharmacol* **81**, 284-91 (2012).

15. Iglesias, T., Waldron, R.T. & Rozengurt, E. Identification of in vivo phosphorylation sites required for protein kinase D activation. *J Biol Chem* **273**, 27662-7 (1998).

16. Matthews, S.A., Rozengurt, E. & Cantrell, D. Characterization of serine 916 as an in vivo autophosphorylation site for protein kinase D/Protein kinase Cmu. *J Biol Chem* **274**, 26543-9 (1999).

17. Waldron, R.T. et al. Activation loop Ser744 and Ser748 in protein kinase D are transphosphorylated in vivo. *J Biol Chem* **276**, 32606-15 (2001).

18. Rozengurt, E. Protein kinase D signaling: multiple biological functions in health and disease. *Physiology (Bethesda)* **26**, 23-33 (2011).

19. Zugaza, J.L., Waldron, R.T., Sinnett-Smith, J. & Rozengurt, E. Bombesin, vasopressin, endothelin, bradykinin, and platelet-derived growth factor rapidly activate protein kinase D through a protein kinase C-dependent signal transduction pathway. *J Biol Chem* **272**, 23952-60 (1997).

20. Van Lint, J., Ni, Y., Valius, M., Merlevede, W. & Vandenheede, J.R. Platelet-derived growth factor stimulates protein kinase D through the activation of phospholipase Cgamma and protein kinase C. *J Biol Chem* **273**, 7038-43 (1998).

21. Abedi, H., Rozengurt, E. & Zachary, I. Rapid activation of the novel serine/threonine protein kinase, protein kinase D by phorbol esters, angiotensin II and PDGF-BB in vascular smooth muscle cells. *FEBS Lett* **427**, 209-12 (1998).

22. Waldron, R.T. & Rozengurt, E. Oxidative stress induces protein kinase D activation in intact cells. Involvement of Src and dependence on protein kinase C. *J Biol Chem* **275**, 17114-21 (2000).

23. Arun, S.N., Kaddour-Djebbar, I., Shapiro, B.A. & Bollag, W.B. Ultraviolet B irradiation and activation of protein kinase D in primary mouse epidermal keratinocytes. *Oncogene* **30**, 1586-96 (2011).

24. Rey, O., Young, S.H., Cantrell, D. & Rozengurt, E. Rapid protein kinase D translocation in response to G protein-coupled receptor activation. Dependence on protein kinase C. *J Biol Chem* **276**, 32616-26 (2001).

25. Matthews, S.A., Iglesias, T., Rozengurt, E. & Cantrell, D. Spatial and temporal regulation of protein kinase D (PKD). *EMBO J* **19**, 2935-45 (2000).

26. Rey, O., Reeve, J.R., Jr., Zhukova, E., Sinnett-Smith, J. & Rozengurt, E. G protein-coupled receptor-mediated phosphorylation of the activation loop of protein kinase D: dependence on plasma membrane translocation and protein kinase Cepsilon. *J Biol Chem* **279**, 34361-72 (2004).

27. Sebolt-Leopold, J.S. & Herrera, R. Targeting the mitogen-activated protein kinase cascade to treat cancer. *Nat Rev Cancer* **4**, 937-47 (2004).

28. Wang, Y. et al. The RAS effector RIN1 directly competes with RAF and is regulated by 14-3-3 proteins. *Mol Cell Biol* **22**, 916-26 (2002).

29. Sinnett-Smith, J., Zhukova, E., Hsieh, N., Jiang, X. & Rozengurt, E. Protein kinase D potentiates DNA synthesis induced by Gq-coupled receptors by increasing the duration of ERK signaling in swiss 3T3 cells. *J Biol Chem* **279**, 16883-93 (2004).

30. Sinnett-Smith, J., Zhukova, E., Rey, O. & Rozengurt, E. Protein kinase D2 potentiates MEK/ERK/RSK signaling, c-Fos accumulation and DNA synthesis induced by bombesin in Swiss 3T3 cells. *J Cell Physiol* **211**, 781-90 (2007).

31. Roberts, P.J. & Der, C.J. Targeting the Raf-MEK-ERK mitogen-activated protein kinase cascade for the treatment of cancer. *Oncogene* **26**, 3291-310 (2007).

32. Martin, M., Kettmann, R. & Dequiedt, F. Class IIa histone deacetylases: regulating the regulators. *Oncogene* **26**, 5450-67 (2007).

33. Vega, R.B. et al. Protein kinases C and D mediate agonist-dependent cardiac hypertrophy through nuclear export of histone deacetylase 5. *Mol Cell Biol* **24**, 8374-85 (2004).

34. Storz, P., Doppler, H., Johannes, F.J. & Toker, A. Tyrosine phosphorylation of protein kinase D in the pleckstrin homology domain leads to activation. *J Biol Chem* **278**, 17969-76 (2003).

35. Storz, P. & Toker, A. Protein kinase D mediates a stress-induced NF-kappaB activation and survival pathway. *EMBO J* **22**, 109-20 (2003).

36. Storz, P., Doppler, H. & Toker, A. Protein kinase Cdelta selectively regulates protein kinase D-dependent activation of NF-kappaB in oxidative stress signaling. *Mol Cell Biol* **24**, 2614-26 (2004).

37. Hurd, C. & Rozengurt, E. Protein kinase D is sufficient to suppress EGF-induced c-Jun Ser 63 phosphorylation. *Biochem Biophys Res Commun* **282**, 404-8 (2001).

38. Hurd, C., Waldron, R.T. & Rozengurt, E. Protein kinase D complexes with C-Jun N-terminal kinase via activation loop phosphorylation and phosphorylates the C-Jun N-terminus. *Oncogene* **21**, 2154-60 (2002).

39. Waldron, R.T., Whitelegge, J.P., Faull, K.F. & Rozengurt, E. Identification of a novel phosphorylation site in c-jun directly targeted in vitro by protein kinase D. *Biochem Biophys Res Commun* **356**, 361-7 (2007).

40. Gschwendt, M. et al. Inhibition of protein kinase C mu by various inhibitors. Differentiation from protein kinase c isoenzymes. *FEBS Lett* **392**, 77-80 (1996).

41. Haworth, R.S. & Avkiran, M. Inhibition of protein kinase D by resveratrol. *Biochem Pharmacol* **62**, 1647-51 (2001).

42. Sharlow, E.R. et al. Potent and selective disruption of protein kinase D functionality by a benzoxoloazepinolone. *J Biol Chem* **283**, 33516-26 (2008).

43. Lavalle, C.R. et al. Novel protein kinase D inhibitors cause potent arrest in prostate cancer cell growth and motility. *BMC Chem Biol* **10**, 5 (2010).

44. Guo, J. et al. In vitro cytotoxicity, pharmacokinetics, tissue distribution, and metabolism of small-molecule protein kinase D inhibitors, kb-NB142-70 and kb-NB165-09, in mice bearing human cancer xenografts. *Cancer Chemother Pharmacol* **71**, 331-44 (2013).

45. George, K.M. et al. Design, Synthesis, and Biological Evaluation of PKD Inhibitors. *Pharmaceutics* **3**, 186-228 (2011).

46. Meredith, E.L. et al. Identification of orally available naphthyridine protein kinase D inhibitors. *J Med Chem* **53**, 5400-21 (2010).

47. Meredith, E.L. et al. Identification of potent and selective amidobipyridyl inhibitors of protein kinase D. *J Med Chem* **53**, 5422-38 (2010).

48. Fielitz, J. et al. Requirement of protein kinase D1 for pathological cardiac remodeling. *Proc Natl Acad Sci U S A* **105**, 3059-63 (2008).

49. Knight, Z.A. & Shokat, K.M. Chemical genetics: where genetics and pharmacology meet. *Cell* **128**, 425-30 (2007).

50. Evans, I.M. et al. Characterization of the biological effects of a novel protein kinase D inhibitor in endothelial cells. *Biochem J* **429**, 565-72 (2010).

51. Harikumar, K.B. et al. A novel small-molecule inhibitor of protein kinase D blocks pancreatic cancer growth in vitro and in vivo. *Mol Cancer Ther* **9**, 1136-46 (2010).

52. Tandon, M. et al. A targeted library screen reveals a new inhibitor scaffold for protein kinase D. *PLoS One* **7**, e44653 (2012).

53. Endicott, J.A., Noble, M.E. & Johnson, L.N. The structural basis for control of eukaryotic protein kinases. *Annu Rev Biochem* **81**, 587-613 (2012).

54. Huse, M. & Kuriyan, J. The conformational plasticity of protein kinases. *Cell* **109**, 275-82 (2002).

55. Dar, A.C. & Shokat, K.M. The evolution of protein kinase inhibitors from antagonists to agonists of cellular signaling. *Annu Rev Biochem* **80**, 769-95 (2011).

56. Zhang, J., Yang, P.L. & Gray, N.S. Targeting cancer with small molecule kinase inhibitors. *Nat Rev Cancer* **9**, 28-39 (2009).

57. Norman, R.A., Toader, D. & Ferguson, A.D. Structural approaches to obtain kinase selectivity. *Trends Pharmacol Sci* **33**, 273-8 (2012).

58. Zuccotto, F., Ardini, E., Casale, E. & Angiolini, M. Through the "gatekeeper door": exploiting the active kinase conformation. *J Med Chem* **53**, 2681-94 (2010).

59. Hubbard, S.R. & Till, J.H. Protein tyrosine kinase structure and function. *Annu Rev Biochem* **69**, 373-98 (2000).

60. Balzano, D., Santaguida, S., Musacchio, A. & Villa, F. A general framework for inhibitor resistance in protein kinases. *Chem Biol* **18**, 966-75 (2011).

61. Bissantz, C., Kuhn, B. & Stahl, M. A medicinal chemist's guide to molecular interactions. *J Med Chem* **53**, 5061-84 (2010).